

UCLA

Adaptive Optics for Extremely Large Telescopes 4 - Conference Proceedings

Title

Implementation of SLODAR atmospheric turbulence profiling to the ARGOS system

Permalink

<https://escholarship.org/uc/item/42h0n70s>

Journal

Adaptive Optics for Extremely Large Telescopes 4 – Conference Proceedings, 1(1)

Authors

Mazzoni, Tommaso

Busoni, Lorenzo

Esposito, Simone

et al.

Publication Date

2015

DOI

10.20353/K3T4CP1131611

Copyright Information

Copyright 2015 by the author(s). All rights reserved unless otherwise indicated. Contact the author(s) for any necessary permissions. Learn more at

<https://escholarship.org/terms>

Peer reviewed

Implementation of SLODAR atmospheric turbulence profiling to the ARGOS system

Tommaso Mazzoni^{a,b}, Lorenzo Busoni^a, Marco Bonaglia^a, Simone Esposito^a

^aINAF Osservatorio Arcetri, L. Enrico Fermi 5, 50125 Firenze, Italy

^bUniversità degli studi di Firenze, P.zza S.Marco 4, 50121 Firenze, Italy

ABSTRACT

ARGOS is the Ground Layer Adaptive Optics system of the Large Binocular Telescope, on each side it uses three Laser Guide Stars, generated by Rayleigh backscattered light of pulsed lasers. Three Shack-Hartmann WFS are used to measure the wavefront distortion in the Ground Layer. The SLOpe Detection And Ranging (SLODAR) is a technique used to measure the atmospheric turbulence profiles. Cross correlation of wavefronts gradients from multiple stars are used to estimate the relative strength of turbulent layers at different altitudes. We present here the first results obtained on sky of applying the SLODAR technique to ARGOS comparing then with a previous study based on end-to-end simulations.

Keywords: Adaptive Optics, atmospheric profiling, simulation

1. ARGOS

ARGOS[1] is the laser guide star adaptive optics facility of the LBT. It makes use of commercial Nd:YAG lasers at 532 nm to produce a constellation of 3 artificial reference sources on both telescope sides. Each LGS is generated by the Rayleigh scattering of air molecules of 18 W light pulses emitted by a laser head. On both sides the 3 laser beams are first expanded and then focused at 12 km distance by the refractive launch optics. The lasers are launched into atmosphere from the back of the adaptive secondaries, producing a triangular constellation of LGS inscribed in a circle of 2' radius centered on the telescope optical axis.

The three WFSs have a Shack-Hartmann configuration sensing the pupil generated by each LGS with 15x15 subapertures and arranging them on a single detector with 248x256 pixels[2]. Because the laser beams are s-polarized it is possible to use electro-optical shutters to range gate the WFS detector. These devices are custom produced Pockels cells, triggered by the emission of the laser pulses and properly synchronized to select a range of 150 m centered on the nominal LGS altitude of 12 km.

The signals measured by the centroiding algorithm of the 3 SH sensors are concatenated to the NGS-based tip-tilt measurement into the ARGOS slope computer and the complete vector is send to the adaptive secondary for the AO reconstruction. By inverting together the 3 interaction matrices recorded between the SH sensors and the adaptive secondary it is possible to calibrate ARGOS as a GLAO system. Indeed with this approach the correlated wavefront component measured by the 3 sensors, hence the turbulence closer to the system pupil, is enhanced while the decorrelated one is washed out by the GLAO reconstructor. The ARGOS telemetry stores the individual signals of the 3 SH sensors at 1 kHz rate, we make use of these data to reconstruct the turbulence profiling aokking the SLODAR technique.

2. SLODAR IMPLEMENTATION WITH ARGOS

The SLOpe Detection And Ranging (SLODAR[3]) is a method to calculate the atmospheric turbulence profile $C_n^2(h)$ using the spatial covariance of the cross-correlation of the measured slopes between WFSs. We implemented a system based on SLODAR method with ARGOS. The SLODAR technique must be modified to be applied to AO system based on multiple laser guide stars and independent WFSs[4][5].

Further author information:

Tommaso Mazzoni, ✉ tmazzoni@arcetri.astro.it

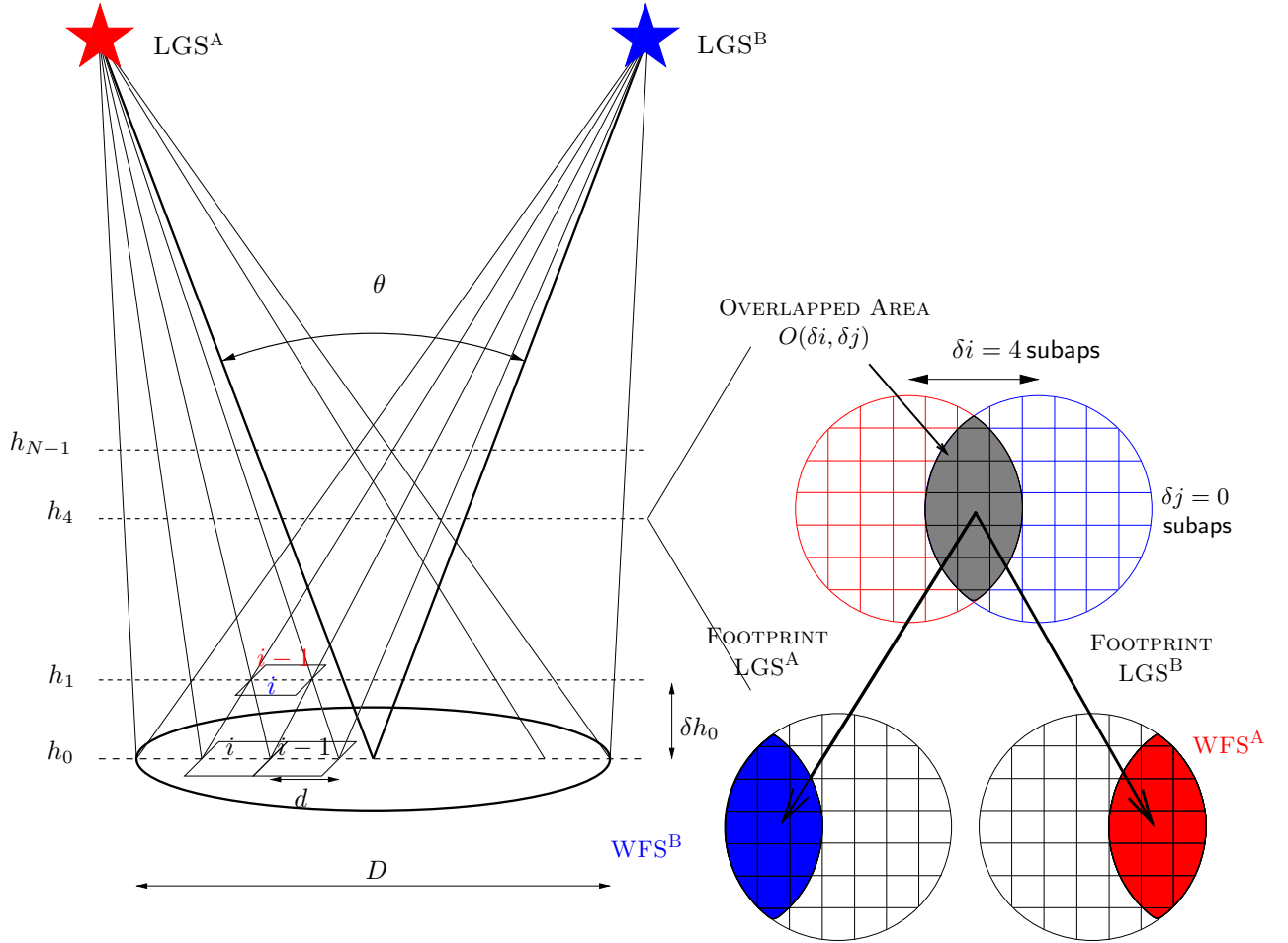


FIGURE 1: Implementation of the SLODAR technique with two laser guide stars (LGS) and two SH (WFS) with 7 subapertures on the diameter. On the right is showed the footprints at altitude h_4 and lower the projection of the overlapped area on the two sensors.

The ARGOS's SLODAR is able estimate the turbulence strength in as many altitude bins as subapertures across the WFSs.

$$h_m = \frac{mdz}{z\theta + md} \quad (1)$$

where $m = 1, 2, \dots, N - 1$ is the selected bin, z is the altitude of the LGS (12 km), θ is the angular distance ($2\sqrt{3}'$), $d = D/N$ is the dimension of a subaperture and N the number of subapertures over the telescope diameter D . At altitude $h_0 = 0$ km the footprints of the three stars are totally overlapped on the telescope, but at h_i only some subapertures are overlapped and the method uses the slopes measured in these subapertures for calculate the spatial covariance. We didn't use the bins over $h_9 = 3187$ m because the overlapped subapertures are too few and the cross-correlation signals are too low.

The cross correlation between two sensor (A and B) in the x direction is given by:

$$C_{sx}(\delta i, \delta j) = \frac{\langle \sum_{i,j} s_x^A(i, j) s_x^B(i + \delta i, j + \delta j) \rangle}{O(\delta i, \delta j)} \quad (2)$$

where s_x is the slopes signal in the x direction, (i, j) are the (x, y) position expressed in subapertures and $O(\delta i, \delta j)$ is the number of overlapped subapertures as function of the distances $(\delta i, \delta j)$. " $\langle \rangle$ " is the temporal

average in a data set.

The autocorrelation of the two sensors is given by the mean of the two autocorrelation signals:

$$\mathcal{A}_{sx}(\delta i, \delta j) = \frac{1}{2} \frac{\langle \sum_{i,j} s^A(i, j) s^A(i + \delta i, j + \delta j) \rangle}{O(\delta i, \delta j)} + \quad (3)$$

$$\frac{1}{2} \frac{\langle \sum_{i,j} s^B(i, j) s^B(i + \delta i, j + \delta j) \rangle}{O(\delta i, \delta j)} \quad (4)$$

The autocorrelation signal is used for a two dimensional deconvolution of the cross correlation signals, like:

$$\mathcal{C}_D = \mathcal{F}^{-1} \left[\frac{\mathcal{F}[\mathcal{C}^{AB}]}{\mathcal{F}[\mathcal{A}/\max(\mathcal{A})]} \right] \quad (5)$$

The autocorrelation is normalized to the maximum because we want preserve the dimensionality.

For the wind profile technique we use the time-delayed cross correlation calculated as:

$$\mathcal{T}_{sx}(\delta i, \delta j, \delta t) = \frac{\langle \sum_{i,j} s_x^A(i, j, t) s_x^B(i + \delta i, j + \delta j, t + \delta t) \rangle}{O(\delta i, \delta j)} \quad (6)$$

where t is the time and δt is a multiple of the acquisition time. With $\delta t = 0$ we obtain the cross correlation of equation 2. Even in this case we apply the Fourier deconvolution:

$$\mathcal{T}_D = \mathcal{F}^{-1} \left[\frac{\mathcal{F}[\mathcal{T}]}{\mathcal{F}[\mathcal{A}/\max(\mathcal{A})]} \right] \quad (7)$$

One of the main aim of this study is to develop a tool to estimate the GLAO performance according to the estimate turbulence profile, and to use it as diagnostic tool during the commissioning of ARGOS at LBT. This implementation of the SLODAR method is insensitive to the turbulence above 12 km and due to the cone effect its sensibility decreases with the altitude.

We can express the *gain* of GLAO system as the ratio between the Full Width Half Maximum (FWHM) of a seeing limited observation and the FWHM of GLAO corrected image. Another way to define a *gain* is as the ratio of the ensquared energy. In the two cases:

$$gain_{FWHM} = \frac{FWHM^{atm}}{FWHM^{corr}}; \quad gain_E = \frac{E^{corr}}{E^{atm}} \quad (8)$$

3. RESULTS FROM SIMULATION

An end-to-end code[6] is used to simulate the ARGOS GLAO system including the computation of the WFS signals that are used for SLODAR turbulence profiling. To speed up the statistical convergence the simulations are performed in open-loop: the distorted phase in the pupil is used to compute the SH spot grid on the CCD frame. The slopes signals are used to reconstruct the sensed ground layer wavefront that is subtracted from the input wavefront. The residual wavefront is stored for PSF computation. A typical simulation run is made of 100-1000 independent atmospheric screens. The $4' \times 4'$ science FoV is sampled with a 5×5 grid and the PSFs of each short-exposure are summed to provide a long-time exposure. The long exposure PSF are analyzed to extract the FWHM and the ensquared Energy in a 0.25 square pixel.

The baseline configuration assumes 3 Rayleigh stars focused at 12km, range-gated over 100 m and arranged on a $2'$ radius circle. To simulate an NGS tip/tilt correction, the overall tip/tilt is subtracted from the wavefront before the LGS sensing is done. The atmospheric phase-screens are generated using the PSG package from the CAOS software [7]. The atmospheric phase-screens are 1024×1024 pixels, 0.046 m/px with outer scale $L_0 = 30$ m. Turbulence strength of each layer is derived by the turbulence profiles measured at Mt Graham[8].

To compare our findings with previous results we used in this study the same C_n^2 profile used during the preliminary study of ARGOS.

From the turbulence measures at Mt Graham we got three median profiles called: 75% , 50% and 25%. The percentages represent the rate of nights considered “bad”, “typical” and “good” in a cumulative distribution of the profile measures. The reconstruction of the three median profiles is showed in Figure 2(a) in terms of J , defined as the integrated profile ($J_m = \int_m C_n^2(h) dh = C_n^2(h_m)\delta h_m$). The distribution of the three profiles is approximately the same but the total strength of the turbulence changes of about a factor 5. The continuous lines are the simulated profiles and the points are the reconstructions performed with the SLODAR technique. Table 1 summarize the results. The reconstruction of the “bad” profile is underestimated because in this case the sensibility of the SH decrease due to the increase of the spot dimension.

Figure 2(b) shows the reconstruction of five profiles with the same total strength ($r_0 \simeq 0.12$ m) but with different vertical distributions. The aim of these simulations is to verify if the technique can distinguish between the cases. The uncertainty estimated is about $\Delta J_m = 5 \times 10^{-15} \text{ m}^1/3$ that is comparable with the strength of a weak turbulent layer.

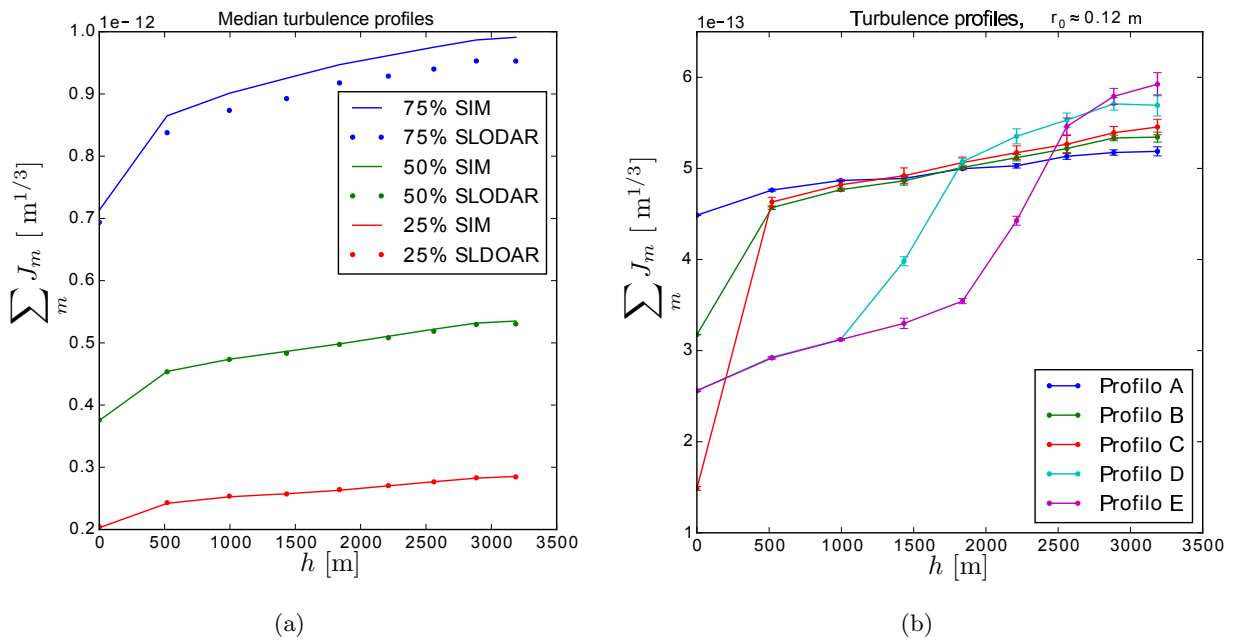


FIGURE 2: Reconstruction of realistic turbulence profiles.

TABLE 1: Fried parameter and “seeing” values used in the simulations ($r_0^{\text{SIM}}, \varepsilon^{\text{SIM}}$) with reconstructed values ($r_0^{\text{MEAS}}, \varepsilon^{\text{MEAS}}$).

Profilo	r_0^{SIM} [m]	r_0^{MEAS} [m]	ε^{SIM} ["]	$\varepsilon^{\text{MEAS}}$ ["]
75%	0.081	0.083	1.251	1.221
50%	0.117	0.118	0.864	0.859
25%	0.171	0.170	0.592	0.591

4. RESULTS ON SKY

In this section we present the results obtained analyzing the data of three nights. The data are blocks of 4000 slopes (acquired in ~ 4 s) and then collected in sets of 3-4 blocks. The nights are classified as 20150227, 20150501 and 20150502. The data have been acquired with DX (right) ARGOS system in “closed-loop” during its commissioning.

Figure 3 shows the reconstructed turbulence profiles in the three nights. The cumulate profiles are the average of period from 20 minutes for the first night to one hour and half for the last night. Altitudes h_m over the telescope are evaluated as:

$$h_m = \left(\frac{mdz}{z\theta + md} + h_p \right) \frac{1}{\sec \zeta} \quad (9)$$

where ζ is the zenith angle and h_p is the altitude at which the pupil is conjugated.

Figure 4 shows the total of the turbulence profiles as function of the measure of the “seeing” performed by the DIMM. J_{DIMM} is total strength of the turbulence calculated as:

$$J_{\text{DIMM}} = \frac{(r_0^{\text{DIMM}})^{-5/3}}{0.423(2\pi/\lambda)^2}; \quad r_0^{\text{DIMM}} = 0.98 \frac{\lambda}{\varepsilon^{\text{DIMM}}} \quad (10)$$

where ε is the measure of the “seeing”, r_0^{DIMM} is the corresponding Fried parameter.

The SLODAR measurement underestimates what is actually the total effect of the turbulence indeed as we already stated in Section 2. We also can't determine the altitude of the layers over $h_9 = 3187$ m, so there is a big uncertainty on the estimation of the residual turbulence measured.

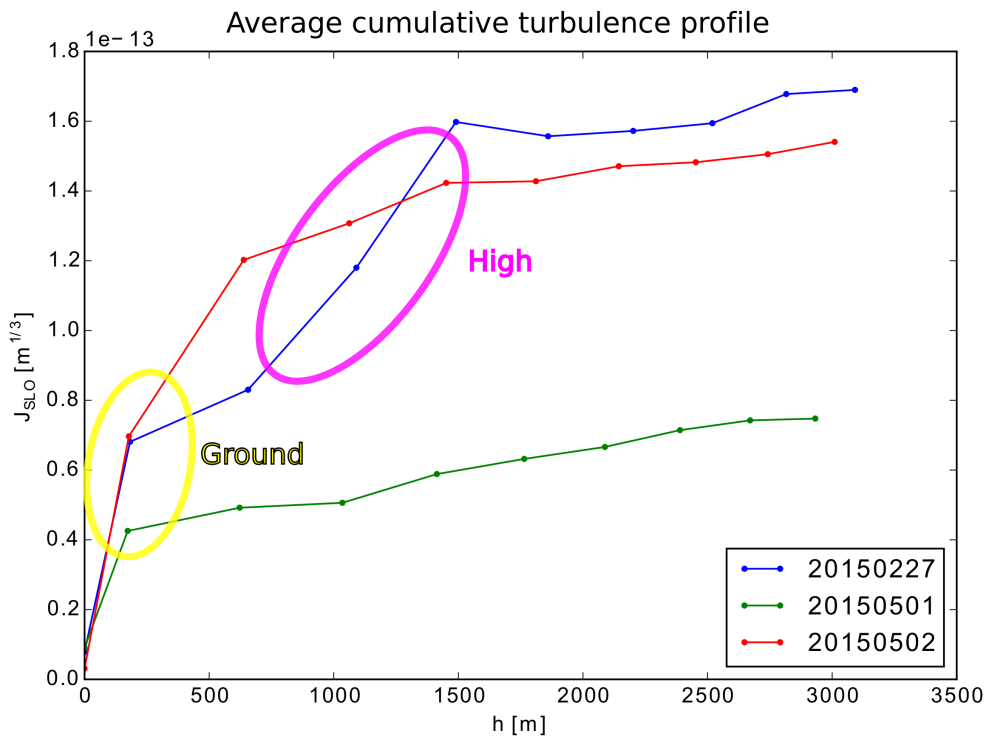


FIGURE 3: Averaged turbulence measured with the SLODAR technique during three nights. In the 20150227 night we identify two separate layers, the first at ground and the second between 1 km and 1.5 km.

DIMM measure vs SLODAR turbulence recostruction ($h < 3\text{km}$)

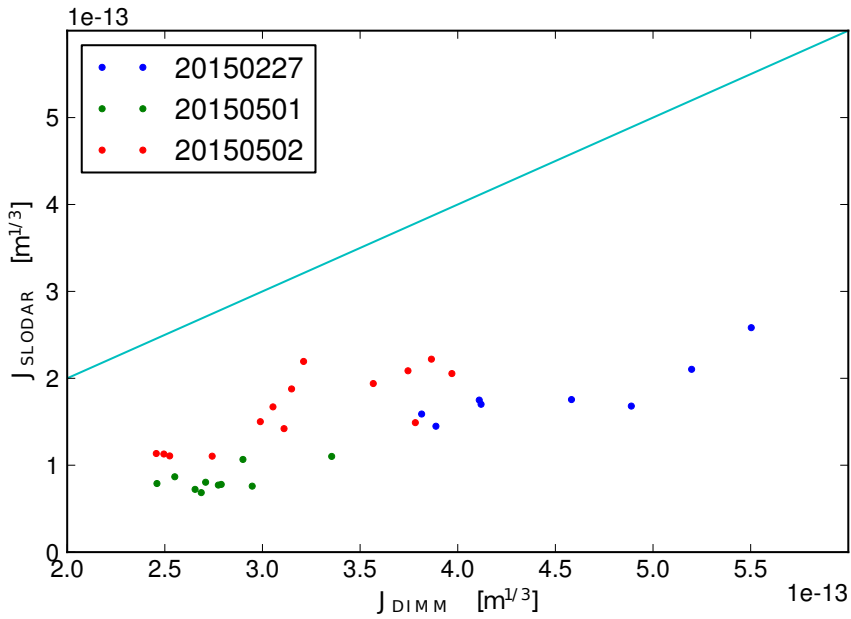


FIGURE 4: Turbulence strength ($h < 3\text{ km}$) measured with the SLODAR technique as function of the DIMM measure.

4.1 Frozen flow

The tracking of the correlation peaks in the time-delayed covariance maps give us information about the movement of the turbulent layers. Basing on Taylor hypothesis the turbulent layers drift with time being moved by the wind like “frozen” layers.

We analyzed with the wind profile technique the higher layer of the night 20150227. Figure 5 shows the evaluated covariance maps. We can identify the higher layer (highlighted in purple) in the map with delay $\delta t = 0.0\text{ s}$. The layer was moving horizontally with respect to the SH sensors geometry. With higher delay we notice a second layer (highlighted in yellow) that was moving, slowly, in another direction. We measure the wind velocity and the wind direction of the higher layer: the results are summarized in the Figures 6. During the observation the wind direction was stable but the speed decrease by 15%. Even the ground layer was identified and the wind speed was $5 \pm 1\text{ m/s}$.

During the observations in the other two nights we identified only the ground layer and the wind speeds were: $4 \pm 1\text{ m/s}$ in the 20150501 night and $5 \pm 1\text{ m/s}$ in the 20150502 night, in agreement with the measures of the telescope’s anemometer ($3.7 \pm 0.5\text{ m/s}$ and $4.6 \pm 0.5\text{ m/s}$).

The time evolution of the peak intensities allows to study the decorrelation of a turbulent layer while it is transported by the wind and then to verify the Taylor hypothesis.

We analyze the layers in the 20150227 night and Figure 7(a) shows the results. The ordinate axis represents the relative intensity (with respect to the zero time) as function of the time delay. The time evolution of the relative intensity represent the decay ratio of the correlation signal. The dashed lines are the best fit and the legend shows the decay ratios expressed in s^{-1} .

The behavior of the dome seeing is like a stationary turbulent layer, so its contribution in the time delayed covariance maps is located at the center. Figure 7(b) shows the decay ratio of the dome seeing, measured at the center of the maps. The ratio decreases quickly because the ground layer correlation peak moves out from the center of the map. The slowly decorrelation (0.3 s^{-1}) is the decay ratio of the dome seeing. Also in this graph the dashed line represent the best fit.

5. CONCLUSIONS

As expected the measures with the SLODAR technique are underestimated respect to the DIMM because the turbulence profiles are reconstructed only below 3 km instead the measures of the DIMM represent the total.

The study of the time-delayed covariance maps had showed that the turbulent layers are not frozen but they decorrelate in less than one second, so only a part of the Taylor's hypothesis is validated. Further measurements will give us a better estimation of the dome seeing and to study the decorrelation of the turbulent layers.

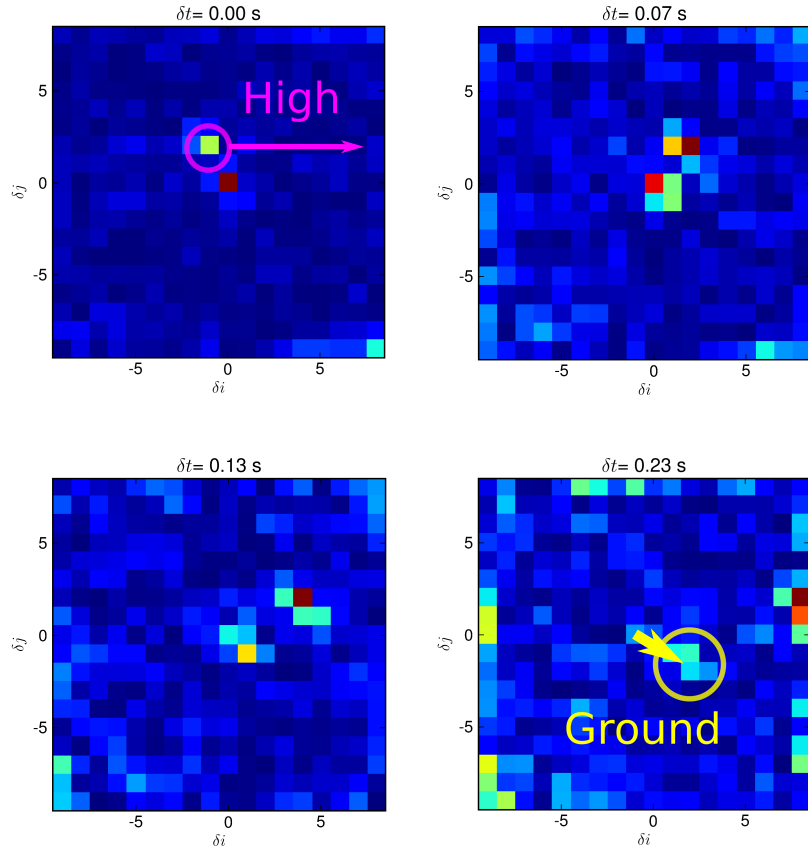
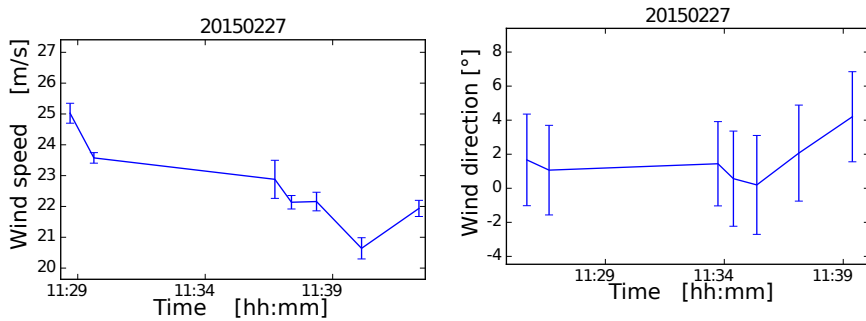


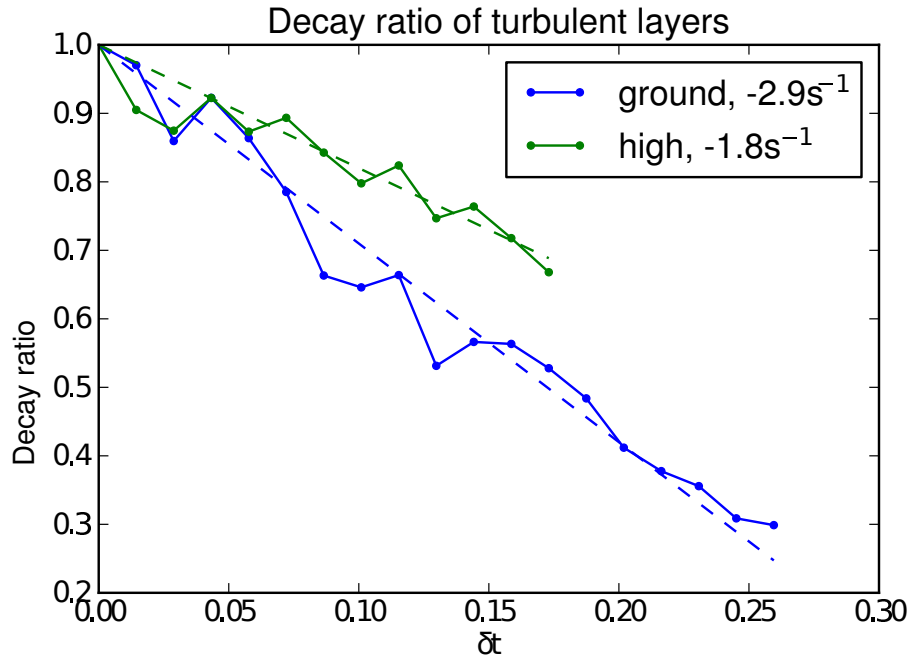
FIGURE 5: Time delayed covariance maps with from da $\delta t=0.0$ s to $\delta t=0.23$ s. Each subapertures ($\delta i=1$) correspond to $d = D/N = 0.55$ m.



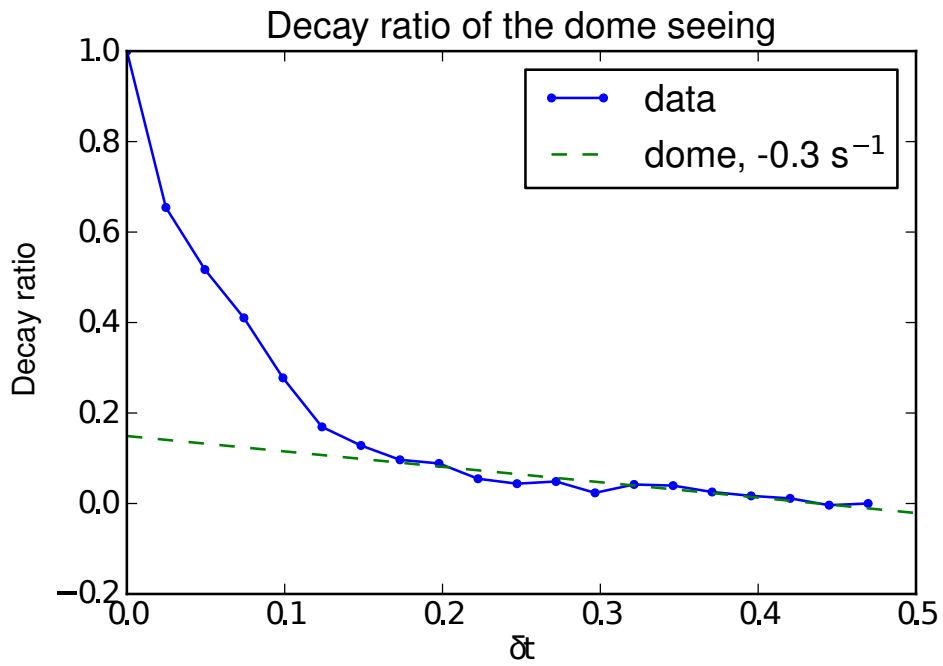
(a) Wind speed.

(b) Wind direction respect to the sensor x axis.

FIGURE 6: Wind measurements in the 20150227 night.



(a) Correlation decay ratio of the two turbulent layers (ground e high) as function of the time delay.



(b) Correlation decay ratio of the dome seeing.

FIGURE 7

REFERENCES

- [1] S. Rabien et al. “ARGOS: the laser guide star system for the LBT”. In: *Proc. SPIE* 7736 (2010), 77360E–77360E–12.
- [2] G. Orban de Xivry et al. “Wide-field AO correction: the large wavefront sensor detector of ARGOS”. In: *Proc. SPIE* 7736 (2010), pp. 77365C–77365C–10.
- [3] R. W. Wilson. “SLODAR : measuring optical turbulence altitude with a Shack-Hartmann wavefront sensor.” In: *Monthly notices of the Royal Astronomical Society*. 337.1 (2002), pp. 103–108.
- [4] A. Cortés et al. “Atmospheric turbulence profiling using multiple laser star wavefront sensors”. In: *Monthly Notices of the Royal Astronomical Society* 427 (Dec. 2012), pp. 2089–2099.
- [5] A. Guesalaga et al. “Using the C_n^2 and wind profiler method with wide-field laser-guide-stars adaptive optics to quantify the frozen-flow decay”. In: *Monthly Notices of the Royal Astronomical Society* 440 (May 2014), pp. 1925–1933.
- [6] L. Busoni et al. “Wavefront sensor for the Large Binocular Telescope laser guide star facility”. In: *Proc. SPIE* 7015 (2008), pp. 701556–701556–11.
- [7] M. Carbillet et al. “Modelling astronomical adaptive optics – I. The software package caos”. In: *Monthly Notices of the Royal Astronomical Society* 356.4 (2005).
- [8] E. Masciadri et al. “Optical turbulence vertical distribution with standard and high resolution at Mt Graham”. In: *Monthly Notices of the Royal Astronomical Society* 404 (2010), pp. 144–158.